On the electronic structure of the ground (X3Σ−) and some low-lying excited states (A3Π, a1Δ, b1Σ+, B3Σ−) of the isovalent species P–Li and P–Na

ARTICLE *in* JOURNAL OF MOLECULAR STRUCTURE THEOCHEM · OCTOBER 1997

Impact Factor: 1.37 · DOI: 10.1016/S0166-1280(97)00146-2

3 AUTHORS:

Demeter Tzeli
National Hellenic Research Foundation
52 PUBLICATIONS **502** CITATIONS
SEE PROFILE

Aristotle Papakondylis
National and Kapodistrian University …
31 PUBLICATIONS **253** CITATIONS
SEE PROFILE

Aristides Mavridis
National and Kapodistrian University …
137 PUBLICATIONS **1,668** CITATIONS
SEE PROFILE

ELSEVIER

Journal of Molecular Structure (Theochem) 417 (1997) 277–287

THEO CHEM

On the electronic structure of the ground ($X^3\Sigma^-$) and some low-lying excited states ($A^3\Pi$, $a^1\Delta$, $b^1\Sigma^+$, $B^3\Sigma^-$) of the isovalent species P-Li and P-Na

Demeter Tzeli, Aristotle Papakondylis, Aristides Mavridis*

National and Kapodistrian University of Athens, Department of Chemistry, Laboratory of Physical Chemistry, P.O. Box 64004, 157 10 Zografou, Athens, Greece

Received 7 October 1996; accepted 2 April 1997

Abstract

The electronic structure of the isovalent P-Li and P-Na species in their ground $X^3\Sigma^-$ state and low-lying excited states, $A^3\Pi$, $a^1\Delta$, $b^1\Sigma^+$ and $B^3\Sigma^-$, has been studied employing CISD, CASSCF and multireference CI techniques. For both molecules and all states studied, we report full potential energy curves, dissociation energies, bond lengths, and spectroscopic constants.

Keywords: P-Li; P-Na; Ab initio; CASSCF-MRCI; Potential curves

1. Introduction

Phosphinidines are compounds of the general form P-X and they can be considered as the second-row analogues of nitrenes, N-X [1]. Although the molecules studied in the present paper, P-Li and P-Na, can be thought as the homologues of the parent phosphinidene, P-H, they are systems of quite different electronic structure.

To the best of our knowledge, no experimental results exist in the literature for the P-Na molecule. Concerning the P-Li system, an experimental dissociation energy, $D = 58.3 \pm 5.5$ kcal mol^{-1} has been reported [2], but as the present calculations and calculations by Simons and co-workers [3,4] indicate, this is overestimated by perhaps as much as 15–20 kcal mol^{-1}. Recently, Boldyrev and Simons [3] reported ab initio calculations on the diatomic systems P-X, X = Li to B, and Na to Si at the SCF/6-31G*, MP2(full)/6-31G*, MP2(full)/6-311 + G* and QCISD(T)/6-311 + G(2df) level of theory. In particular, for the P-Li and P-Na species, these workers examined the $^3\Sigma^-(\sigma^2\pi^2)$, $^3\Pi(\sigma^1\pi^3)$ and $^1\Sigma^+(\pi^4)$ states. As far as we know, no other ab initio calculations exist in the literature for these two molecules.

In the present work, we have examined the states $X^3\Sigma^-(\sigma^2\pi^2)$, $A^3\Pi(\sigma^1\pi^3)$, $a^1\Delta(\sigma^2\pi^2)$, $b^1\Sigma^+(\sigma^2\pi^2)$ and $B^3\Sigma^-(\sigma^{*2}\pi^2)$ of the isovalent P-Li and P-Na systems, mainly via CASSCF (complete active space SCF) and CASSCF + 1 + 2 (CASSCF + single + double replacements = MRCI) employing large basis sets. For all states examined and for both molecules, full potential energy curves (PEC) have been constructed at the MRCI level of theory. This study can

* Corresponding author.

PII S0166-1280(97)00146-2

be considered as a continuation of our work on the analogous species N-Li [5], and following this work we are trying to analyze our findings using simple valence bond-Lewis diagrams.

2. Basis sets and methods

For the Li and P atoms, the correlation consistent polarized valence (cc-pVxZ) basis sets of Dunning were employed [6,7] with x = Q, that is of quadruple quality, but with the functions of g-symmetry removed (cc-pVQZ-g). For the Na atom, the ANO basis set of Roos and co-workers [8] was selected, practically of the same quality as those of the Li and P sets. In summary, the basis sets run as follows, Li: (12s6p3d2f) contracted to [5s4p3d2f], P: (16s11p3d2f) → [6s5p3d2f], Na: (17s12p5p4f) → [5s4p3d2f]. For both P-Li and P-Na molecules, the total number of contracted spherical Gaussian functions is 96. Anticipating the ionic nature of those molecules, the augmented cc-pVQZ-g (cc-pVQZ + one diffuse function for each symmetry present) was also used for the P atom and for the P-Li species. The obtained differences on bond length and dissociation energy D_e were not significant (vide infra), therefore this approach was not pursued any further. Judging the basis set sizes to be quite adequate, basis set superposition error corrections were not taken into account.

Results reported in the present work are based on SCF, CISD (SCF + 1 + 2), CASSCF and CASSCF + 1 + 2 (MRCI) wave functions. In all correlated calculations "core" electrons, i.e. $\sim 1s^2$ on Li, $\sim 1s^2 2s^2 2p^6$ on Na and P were kept frozen, allowing excitations from the six valence electron molecular space only. The CAS wave functions were constructed by allowing all possible excitations out of the 6 e^- valence (active) space into six appropriate orbitals. Specifically, every doubly occupied orbital describing a bond or a "lone pair" on the P-atom was provided with an additional antibonding orbital of the proper symmetry; no extra functions were provided for the singly occupied orbitals. For example, approximating such a CAS wave function in a GVB way, the $X^3\Sigma^-$ state of PLi (or PNa) is written:

$$|X^3\Sigma^-\rangle_{GVB} = \mathcal{A}(\text{core})^{12}(1\sigma^2 - \lambda 2\sigma^{*2}) \times (3\sigma^2 - \mu 4\sigma^{*2})\pi_x^1 \pi_y^1 \alpha\beta\alpha\beta\alpha\alpha$$

For the symmetries $^3\Sigma^-$, $^3\Pi$, $^1\Delta$ and $^1\Sigma^+$, the CAS wave functions are comprised of 51, 51, 35 and 60 CSFs respectively, with corresponding MRCI spaces ranging from ~150 000 to 250 000 CSFs.

From the CASSCF and MRCI results, bond distances, r_e, and spectroscopic constants, ω_e (harmonic frequency), $\omega_e x_e$ (first anharmonicity constant), a_e (rotational–vibrational constant) and $\bar{D}_e$ (centrifugal distortion), were calculated by fitting the PECs up to ~6.0 bohr to a seventh degree polynomial and then applying standard Dunham analysis. Finally, dipole moments at the CASSCF and MRCI levels were obtained by placing two unit charges of opposite sign equidistantly from the middle of the bond length. This configuration of unit charges creates an essentially uniform and very weak electric field in the molecular region and along the molecular axis. The distances employed, measured from the middle of the internuclear axis, were 50, 75, 100, 150 and 170 bohr, the plus-unit charge being located from the P-side while the minus-unit charge was located from the Li (or Na) side of the molecule. Dipole moments were obtained as limiting values of the ratio $\Delta E/\Delta\mathcal{E}$ ("derivatives"), where ΔE are total energy differences and $\Delta\mathcal{E}$ are electric field differences. Of course, ΔE values used do not contain the Coulombic attraction of the two opposite charges, but represent energy differences due to the polarization of the molecule(s) in the presence of the electric field. The dipole moments given in the present paper are in essence the results of ΔE and $\Delta\mathcal{E}$ differences as obtained from the 150 to 170 bohr increment. CISD dipole moments were obtained as expectation values of the dipole moment operator.

Our calculations were performed by the COLUMBUS [9] and MELD [10] suites of codes.

3. Results and discussion

In the four excited molecular states examined in the present report, the first two excited states ^2D and ^2P of the P atom, and/or the ^2P state of the alkali metals M (M = Li, Na) are entailed. It is, therefore, of importance that the corresponding atomic energy separations are calculated accurately. These splittings are presented in Table 1. While for the Li atom the

Table 1
Experimental versus theoretical atomic energy separations ΔE (eV) of Li, Na and P atoms

Atom	Li	Na	P	
ΔE	$^2P \leftarrow ^2 S$	$^2P \leftarrow ^2 S$	$^2D \leftarrow ^4 S$	$^2P \leftarrow ^2 D$
SCF	1.841	1.973	1.793	1.321
CISD			1.520	0.976
CASSCF			1.263	1.320
MRCI			1.484	0.942
Expt.[a]	1.846	2.104	1.410	0.913

[a] Ref. [11], averaged values over M_j.

separation $^2P \leftarrow ^2 S$ is in excellent agreement with the experimental value [11], the corresponding result for the Na atom deviates from the experimental value by as much as 3 kcal mol^{-1}. A CISD calculation involving all electrons of the Na atom improves this difference by 1.24 kcal mol^{-1}. For the P atom, the agreement in the $^2D \leftarrow ^4 S$ and $^2P \leftarrow ^2 D$ energy separations can be considered as fair at the MRCI level.

Table 2 and Table 3 present absolute energies, bond distances, dissociation energies (D_e, or intrinsic bond strengths) and energy gaps T_e for the P-Li and P-Na at the SCF, CISD, CASSCF, MRCI and MRCI + Q (MRCI + Davidson corrections [12,13]). For reasons of comparison, for the $X^3\Sigma^-$ and $A^3\Pi$ states, results from Boldyrev and Simons [3] are also included. Table 4 contains the spectroscopic constants ω_e, $\omega_e x_e$, α_e and $\bar{D}_e$ for both systems. In Table 2 and Table 3, some comments are also included, indicating leading configurations and asymptotic products. Full PECs at the MRCI level and for all states are shown in Fig. 1 and Fig. 2; it should be mentioned at this point that all our MRCI PECs are size extensive within a fraction of a *m*hartree. In what follows, and for reasons of clarity, we discuss every state separately.

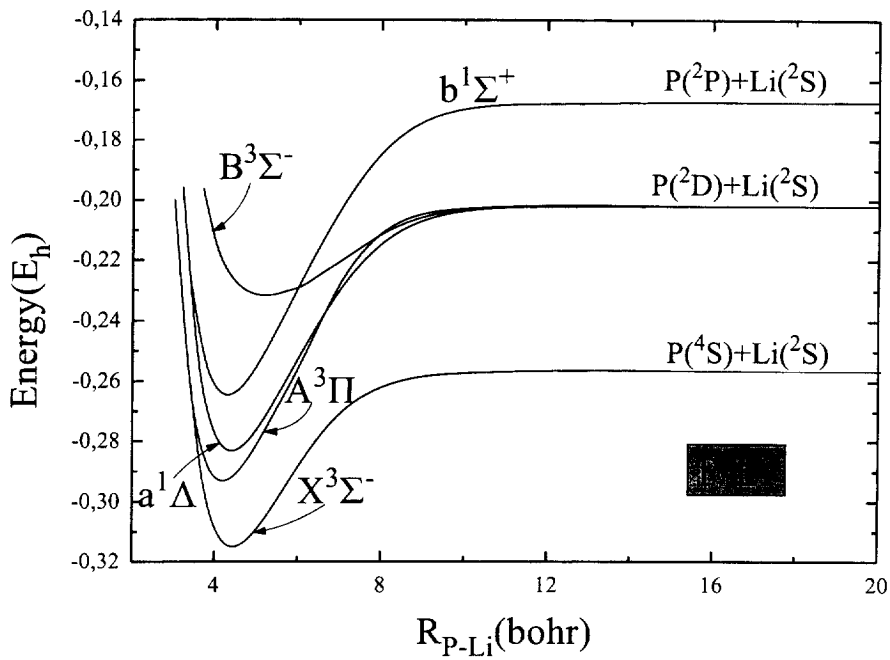

Fig. 1. MRCI potential energy curves of the P-Li molecule.

Table 2
Absolute energies E (hartrees), bond distances r_e (Å), dissociation energies D_e (kcal mol^{-1}), dipole moments μ (D), Mulliken charges q (P) and energy gaps T_e (kcal mol^{-1}) of the $X^3\Sigma^-$, $A^3\Pi$, $a^1\Delta$, $b^1\Sigma^+$ and $B^3\Sigma^-$ states of P-Li molecule

Method	$-E$	r_e	D_e	μ	q(P)	T_e [a]	Comments (leading configurations and asymptotic products)
$X^3\Sigma^-$							
SCF	348.17405	2.342	14.4	7.35	−0.50	0.0	$\|\sigma^2\pi_x^1\pi_y^1\rangle$
CISD	348.30920	2.339	34.2	7.15	−0.47	0.0	
CISD + Q[b]	348.321	2.344	37.4			0.0	
CASSCF	348.19915	2.398	21.5	6.96[f]	−0.43	0.0	$P(^4S)+Li(^2S)$
MRCI	348.31497	2.351	36.8	7.01		0.0	
MRCI + Q[c]	348.324	2.350	39			0.0	
QCISD(T)[d]	348.30484	2.342	38.4			0.0	
$A^3\Pi$							
SCF	348.14970	2.227	40.5	6.71	−0.49	15.3	$\|\sigma^1\pi^3\rangle$
CISD	348.28601	2.219	54.7	6.59	−0.47	14.6	$P(^2D)+Li(^2S)$
CISD + Q[b]	348.299	2.223	57.9			13.8	
CASSCF	348.18098	2.215	40.2	6.68[f]	−0.42	11.4	Avoided crossing between a $^3\Pi$ state correlating to $P(^4S)+Li(^2P, M_L=\pm 1)$ and the one which correlates to $P(^2D)+Li(^2S)$
MRCI	348.29310	2.221	57.3	6.55		13.7	
MRCI + Q[c]	348.301	2.227	60			14.4	
QCISD(T)[e]	348.28182	2.189				14.4	
$a^1\Delta$							
SCF	348.13564	2.332	31.7	7.24	−0.48	24.1	$\|\sigma^2\bar{\pi}_x^1\pi_y^1\rangle-\|\sigma^2\pi_x^1\bar{\pi}_y^1\rangle$
CISD	348.27599	2.327	48.4	7.03	−0.45	20.8	
CISD + Q[b]	348.289	2.328	51.6			20.1	
CASSCF	348.17166	2.366	33.4	7.04[f]	−0.44	17.3	$P(^2D)+Li(^2S)$
MRCI	348.28317	2.332	51.0	6.96		20.0	
MRCI + Q[c]	348.291	2.334	53			20.7	
$b^1\Sigma^+$							
SCF	348.09356	2.327	35.7	6.99	−0.41	50.5	$\|\sigma^2\pi_x^2\rangle+\|\sigma^2\pi_y^2\rangle$
CISD	348.25085	2.302	55.3	6.81	−0.41	36.6	
CISD + Q[b]	348.272	2.278	61.8			30.7	
CASSCF	348.13164	2.345	38.7	6.69[f]	−0.41	42.4	$P(^2P)+Li(^2S)$
MRCI	348.26450	2.281	61.1	6.57		31.7	
MRCI + Q[c]	348.277	2.278	65			29.5	
$B^3\Sigma^-$							
CASSCF	348.12836	2.621	6.21	−1.91[f]	−0.10	44.4	$\|\sigma^{*2}\pi_x^1\pi_y^1\rangle$
MRCI	348.23170	2.746	18.7	−3.42		52.3	$P(^2D)+Li(^2S)$
MRCI + Q[c]	348.241	2.986	22			52.1	

[a] With respect to the $X^3\Sigma^-$ state.
[b] Davidson correction for unlinked quadruples [12].
[c] Multireference Davidson correction for higher than double excitations [13].
[d] Ref. [3], QCISD(T)/6-311 + G(2df).
[e] Ref. [3], QCISD(T)/6-311 + G(2df)//MP2(full)/6-311 + G*.
[f] Calculated at the MRCI bond distance.

Table 3
Absolute energies E (hartrees), bond distances r_e (Å), dissociation energies D_e (kcal mol^{-1}), dipole moments μ (D), Mulliken charges q (P) and energy gaps T_e (kcal mol^{-1}) of the $X^3\Sigma^-$, $A^3\Pi$, $a^1\Delta$, $b^1\Sigma^+$ and $B^3\Sigma^-$ states of P-Na molecule

Method	$-E$	r_e	D_e	μ	q(P)	T_e [a]	Comments (leading configurations and asymptotic products)
$X^3\Sigma^-$							
SCF	502.58208	2.685	3.5	8.70	−0.34	0.0	$\|\sigma^2\pi_x^1\pi_y^1\rangle$
CISD	502.71688	2.689	23.0	8.42	−0.33	0.0	
CISD + Q[b]	502.729	2.699	26.4			0.0	
CASSCF	502.61010	2.771	12.4	7.15[f]	−0.33	0.0	$P(^4S)+Na(^2S)$
MRCI	502.72356	2.710	26.2	7.98		0.0	
MRCI + Q[c]	502.733	2.710	28			0.0	
QCISD(T)[d]	502.70198	2.690	27.8			0.0	
$A^3\Pi$							
SCF	502.56060	2.588	31.3	9.12	−0.43	13.5	$\|\sigma^1\pi^3\rangle$
CISD	502.69567	2.587	44.8	9.03	−0.41	13.3	$P(^2D)+Na(^2S)$
CISD + Q[b]	502.708	2.593	47.5			13.2	
CASSCF	502.59044	2.578	30.2	9.16[f]	−0.44	12.3	Avoided crossing between a $^3\Pi$ state correlating to $P(^4S)+Na(^2P, M_L = \pm 1)$ and the one which correlates to $P(^2D)+Na(^2S)$
MRCI	502.70251	2.589	47.3	9.00		13.2	
MRCI + Q[c]	502.711	2.596	50			13.8	
QCISD(T)[e]	502.67948	2.545				14.1	
$a^1\Delta$							
SCF	502.54306	2.680	20.3	8.74	−0.32	24.5	$\|\sigma^2\bar{\pi}_x^1\pi_y^1\rangle-\|\sigma^2\pi_x^1\bar{\pi}_y^1\rangle$
CISD	502.68267	2.678	36.6	8.54	−0.31	21.5	
CISD + Q[b]	502.695	2.686	39.3			21.3	
CASSCF	502.58036	2.724	22.9	8.10[f]	−0.37	18.7	$P(^2D)+Na(^2S)$
MRCI	502.68991	2.692	39.3	8.30		21.1	
MRCI + Q[c]	502.698	2.694	42			22.0	
$b^1\Sigma^+$							
SCF	502.50004	2.680	23.8	8.75	−0.35	51.5	$\|\sigma^2\pi_x^2\rangle+\|\sigma^2\pi_y^2\rangle$
CISD	502.65661	2.665	42.9	8.65	−0.37	37.8	
CISD + Q[b]	502.678	2.639	49.5			32.0	
CASSCF	502.54055	2.702	28.4	8.04[f]	−0.35	43.6	$P(^2P)+Na(^2S)$
MRCI	502.67158	2.637	49.6	8.57		32.6	
MRCI + Q[c]	502.684	2.637	54			30.7	
$B^3\Sigma^-$							
CASSCF	502.54421	3.037	0.21	1.36[f]	−0.20	41.3	$\|\sigma^{*2}\pi_x^1\pi_y^1\rangle$
MRCI	502.65310	3.188	16.2	−0.41		44.2	$P(^2D)+Na(^2S)$
MRCI + Q[c]	502.665	3.487	21			42.7	

[a] With respect to the $X^3\Sigma^-$ state.
[b] Davidson correction for unlinked quadruples [12].
[c] Multireference Davidson correction for higher than double excitation [13].
[d] Ref. [3], QCISD(T)/6-311 + G(2df).
[e] Ref. [3], QCISD(T)/6-311 + G(2df)//MP2(full)/6-311 + G*.
[f] Calculated at the MRCI bond distance.

Table 4
Spectroscopic constants ω_e, $\omega_e\chi_e$, α_e and $\bar{D}_e$ in cm^{-1} of the $X^3\Sigma^-$, $A^3\Pi$, $a^1\Delta$, $b^1\Sigma^+$ and $B^3\Sigma^-$ states of P-Li and P-Na molecules

Method	P-Li				P-Na			
	ω_e	$\omega_e\chi_e$	$\alpha_e \times 10^{-3}$	$\bar{D}_e \times 10^{-7}$	ω_e	$\omega_e\chi_e$	$\alpha_e \times 10^{-3}$	$\bar{D}_e \times 10^{-7}$
$X^3\Sigma^-$								
CASSCF	439.2	3.9	6.5	−2.8	295.8	3.3	3.4	−8.2
MRCI	479.1	3.3	5.9	−2.6	337.6	2.1	2.5	−7.2
MP2(full)[a]	495				298			
$A^3\Pi$								
CASSCF	523.5	3.3	6.4	−3.2	370.6	2.0	2.7	−8.1
MRCI	514.5	3.5	6.6	−3.2	361.9	2.0	2.7	−8.2
MP2(full)[a]	541				307			
$a^1\Delta$								
CASSCF	470.1	4.0	6.2	−2.6	294.8	−0.4	4.5	−9.0
MRCI	499.4	3.2	5.6	−2.6	337.8	−0.06	2.3	−7.4
$b^1\Sigma^+$								
CASSCF	474.6	3.5	5.6	−2.7	335.9	2.0	2.4	−7.4
MRCI	508.5	3.3	5.4	−2.8	358.9	1.8	2.1	−7.5
$B^3\Sigma^-$								
CASSCF	291.5	2.3	6.5	−3.7	208.3	1.0	2.7	−9.7
MRCI	248.5	8.8	8.2	−3.9	204.0	4.4	1.1	−7.4

[a] Ref. [3], 6-311 + G* basis.

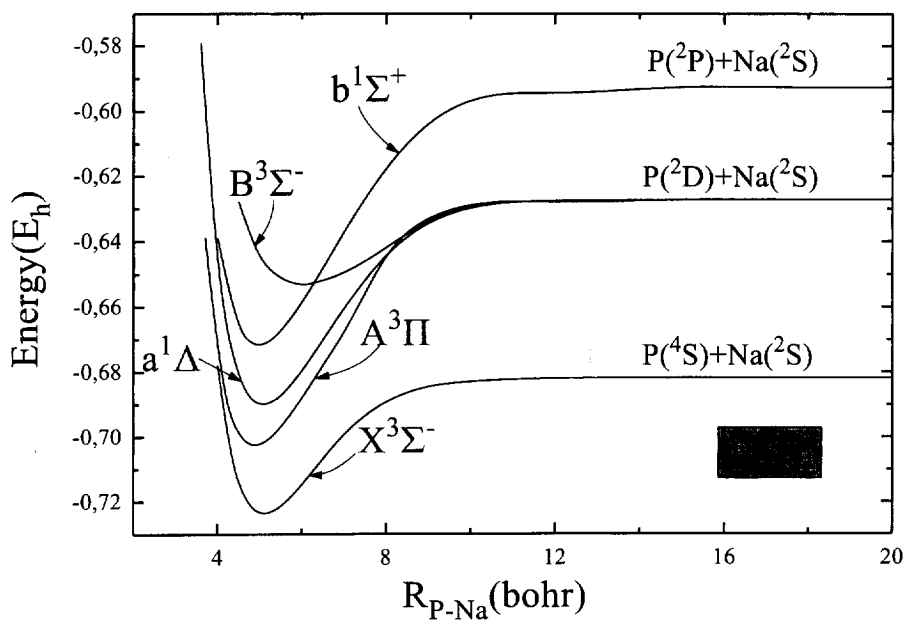

Fig. 2. MRCI potential energy curves of the P-Na molecule.

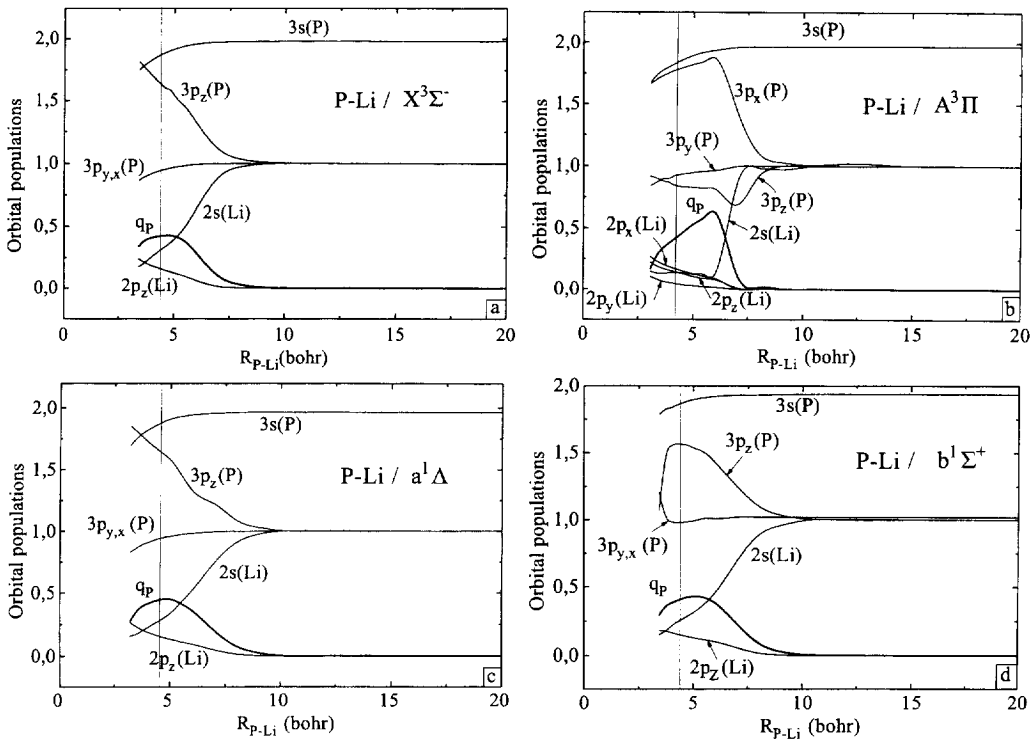

Fig. 3. Evolution of orbital populations and of the charge on the P atom (q_P) along the reaction path of the P-Li molecule, as obtained from the CAS wavefunctions. The perpendicular lines mark the equilibrium bond lengths. (a) $X^3\Sigma^-$, (b) $A^3\Pi$, (c) $a^1\Delta$, (d) $b^1\Sigma^+$.

3.1. $X^3\Sigma^-$ ground state (P-Li, P-Na)

The following valence bond-Lewis icon represents the bond formation of the P-M (M = Li or Na) system from the ground state atoms.

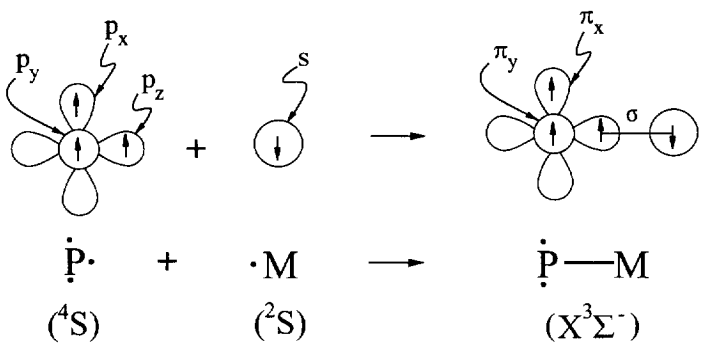

As we can see from the population analysis (Table 3), both molecules present a considerable ionic character with 0.5 e^- and 0.3 e^- transferred from the alkali metal to P in P-Li and P-Na respectively. This ionicity is reflected in the very high dipole moments, 7.0 (P-Li) and 8.0 (P-Na) debye at the MRCI level of theory. By using the augmented basis set on the P atom (aug-cc-pVQZ-g) and for the P-Li molecule, at the MRCI level the total energy drops by 0.6 mh, the

bond length increases by 0.002 Å and the D_e increases by 0.3 kcal mol^{-1}. Judging these differences as insignificant considering the additional computational effort, the aug-basis set was not used any further.

At the equilibrium bond distance, the atomic populations as obtained from the CAS wavefunction are as follows

$$P-Li: 3s^{1.88}3p_{x,y}^{0.95}3p_z^{1.62}/2s^{0.33}2p_{x,y}^{0.03}2p_z^{0.15}$$

$$P-Na: 3s^{1.91}3p_{x,y}^{0.97}3p_z^{1.46}/3s^{0.49}3p_{x,y}^{0.01}3p_z^{0.09}$$

where the first entry corresponds to the P and the second to the Li or Na atom. How the atomic populations evolve, from infinity (~20 bohr) to equilibrium, is shown in Fig. 3(a) for the P-Li species; also shown is the charge build up on the P atom (q_P). For instance, already at the distance of ~7.5 bohr the $3p_z$(P) starts gaining electrons, while at the same time the population of the 2s(Li) is plummeting in a fashion almost symmetric to the $3p_z$(P). A small fraction of electrons is also promoted to the $2p_z$ orbital of Li. The situation is completely analogous for the P-Na system.

Although the HF configuration in the CISD expansion carries a significant weight, $C_{HF}=0.95$ for both molecules, the SCF method essentially fails to predict a reasonable binding energy, particularly for the P-Na molecule (Table 3) where almost all binding energy is correlation energy. From Table 2 and Table 3, we also observe that our r_e's and D_e's are in essential agreement with the results of Boldyrev and Simons [3].

3.2. $A^3\Pi$ state (P-Li, P-Na)

We can think of this state as the result of interaction between the ground ^4S of P and the first excited ^2P ($M_L=\pm 1$) of Li or Na atoms.

This diagram suggests that the molecules are held together by a π-bond, a half σ-bond and a half π-bond. In essence, the CAS population analysis at equilibrium supports this diagram:

$$P-Li: 3s^{1.88}3p_x^{1.78}3p_y^{0.92}3p_z^{0.84}/2s^{0.14}2p_x^{0.17}2p_y^{0.05}2p_z^{0.14}$$

$$P-Na: 3s^{1.85}3p_x^{1.80}3p_y^{0.93}3p_z^{0.83}/3s^{0.15}3p_x^{0.11}3p_y^{0.03}3p_z^{0.11}$$

the total result being the transfer of ~0.4 e^- from Li or Na to the P atom (Table 2 and Table 3).

At equilibrium, the situation is similar to that of N-Li molecule [5]. However, the PECs of this $A^3\Pi$ state, Fig. 1 and Fig. 2, correlate to the first excited ^2D ($|xy\bar{y}\rangle - |xz\bar{z}\rangle$, $M_L=\pm 1$) and ^2S states of P and Li or Na atoms respectively. This in turn suggests an avoided crossing between a $^3\Pi$ strongly bound state originating from the ^4S and ^2P states of P and Li atoms, and a rather weakly bound $^3\Pi$ state tracing its lineage to ^2D and ^2S states of P and Li atoms respectively. The cause of this avoided crossing is, obviously, the intervening ^2D state of P atom between the ^2S and ^2P states of Li or Na atoms (Table 1). Such a situation does not arise in the N-Li system [5] due to the fact that the N ^2D state is *higher* by 0.538 eV (0.280) than the ^2P state of Li (Na) atom. For purely technical reasons, we were not able to compute the assumed $B^3\Pi$ state correlating to the ^4S and ^2P states of P and Li or Na atoms, but corroborating our suggestion are the large D_e values, 57.3 and 47.3 kcal mol^{-1} at the MRCI level of P-Li and P-Na respectively (Table 2 and Table 3) and the shortening by ~0.12 Å of the bond lengths of the $A^3\Pi$ states as compared with corresponding $X^3\Sigma^-$ states (Table 2 and Table 3) for both molecules. It is difficult to interpret such strong interactions as originating between a ^2D(P) and ^2S(Li or Na) states. In addition, calculating the bond dissociation energy of the P-Li molecule with respect to ^4S(P) and ^2P(Li) asymptotic

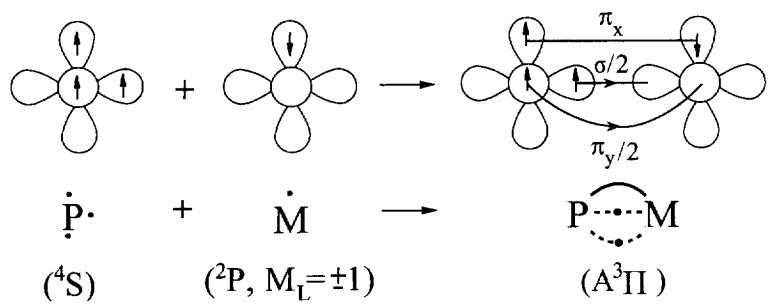

products (intrinsic bond strength), we obtain a value of 65.5 kcal mol^{-1} at the MRCI level, with the corresponding value of the N-Li system [5] being 64.6 kcal mol^{-1}. The fact that the two intrinsic bond strengths are practically the same between the $A^3\Pi$ states of P-Li and N-Li molecules suggests that their binding mechanisms are similar, and clearly the latter correlates to the ^4S and ^2P states of N and Li atoms.

Fig. 3(b) shows the evolution of atomic populations, as obtained from the CAS wavefunction along the PEC for the P-Li species; for P-Na the results are strictly similar.

Finally, from Table 2 and Table 3, we can see that our T_e ($A^3\Pi \leftarrow X^3\Sigma^-$) values of 13.7 (14.4) and 13.2 (13.8) kcal mol^{-1} at the MRCI (MRCI + Q) level of P-Li and P-Na are in essential agreement with the results of Boldyrev and Simons [3] (14.4 and 14.1 kcal mol^{-1}, QCISD(T) level). What is different though, between our results and the results of Ref. [3] is the bond lengths, ours being longer by 0.032 and 0.044 Å for P-Li and P-Na respectively. The cause of this discrepancy is the MP2(full) methodology and the rather small basis set (6-311 + G*) used by these workers [3] as contrasted to the MRCI approach and much larger basis used in the present work.

3.3. $a^1\Delta$ state (P-Li, P-Na)

This state originates from a $\sigma^2\pi^2$ configuration and correlates to the ^2D and ^2S states of P and Li or Na atoms respectively (Fig. 1 and Fig. 2). The equilibrium structure can be represented with the following valence bond-Lewis diagram.

In addition, the CAS atomic populations at the equilibrium are

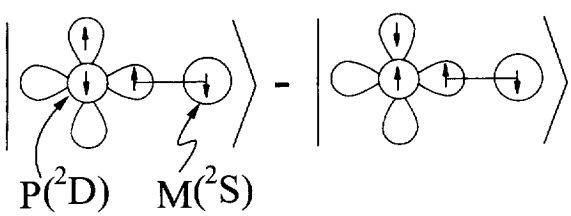

$$P-Li: 3s^{1.87}3p_{x,y}^{0.94}3p_z^{1.65}/2s^{0.28}2p_{x,y}^{0.03}2p_z^{0.16}$$

$$P-Na: 3s^{1.88}3p_{x,y}^{0.95}3p_z^{1.56}/3s^{0.40}3p_{x,y}^{0.02}3p_z^{0.16}$$

while the evolution of the atomic populations along the PEC of P-Li are shown in Fig. 3(c); the corresponding evolutional diagram for P-Na is quite similar. The bonding is clearly caused by a significant electron transfer from the s orbitals of the alkali metals to the p_z orbital of the P atom, with a concomitant promotion of $\sim 0.20e^-$ to the $2p_z$ and $3p_z$ of Li and Na respectively, resulting in a total transfer of $\sim 0.4\ e^-$ from Li or Na to P (Table 2 and Table 3). How the charge is accumulated on the P atom of the P-Li system along the reaction coordinate is shown in Fig. 3(c).

Both the $A^3\Pi$ and the $a^1\Delta$ states of P-Li and P-Na species are bound with respect to the ground state products by 23.1, 16.9 and 13.0, 5.1 kcal mol^{-1} respectively. The similarity of bonding between the $X^3\Sigma^-$ and $a^1\Delta$ states (a difference of a spin flip between the two states), is reflected in the similarity of bond distances, charge transfer and dipole moments of these states for both species (Table 2 and Table 3).

3.4. $b^1\Sigma^+$ state (P-Li, P-Na)

This $^1\Sigma^+$ state also originates from a $\sigma^2\pi^2$ configuration, tracing its lineage to the second excited state of the P atom, ^2P and the ground state of the alkali metals, ^2S. At equilibrium, it can be represented with the following valence bond-Lewis picture and with the following atomic CAS populations

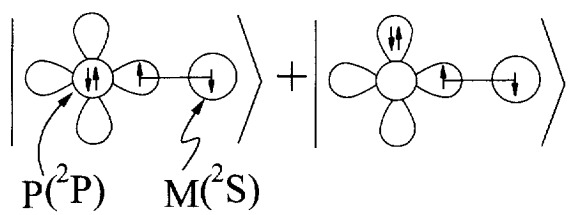

$$P-Li: 3s^{1.87}3p_{x,y}^{0.98}3p_z^{1.57}/2s^{0.26}2p_{x,y}^{0.07}2p_z^{0.15}$$

$$P-Na: 3s^{1.88}3p_{x,y}^{1.00}3p_z^{1.47}/3s^{0.35}3p_{x,y}^{0.04}3p_z^{0.11}$$

The evolution of the atomic populations along the

P-Li curve is shown in Fig. 3(d). A total charge of ~0.4 e^- is again transferred from the Li or Na atom to the P atom (see Table 2 and Table 3) mainly through the σ-frame of the molecules along with a small promotion to the $2p_z$ and $3p_z$ orbitals of Li and Na atoms.

Of the three states $X^3\Sigma^-$, $a^1\Delta$ and $b^1\Sigma^+$ stemming from the $\sigma^2\pi^2$ configuration and at the MRCI level, the $b^1\Sigma^+$ state has the shortest bond distance and the highest dissociation energy (intrinsic bond strength) with respect to the adiabatic fragments, $P(^2P)$ and Li or Na (^2S). The same situation holds for the N-Li molecule as well [5].

3.5. $B^3\Sigma^-$ state (P-Li, P-Na)

Fig. 1 and Fig. 2 present the $B^3\Sigma^-$ PECs of the P-Li and P-Na molecules. As shown, both systems correlate adiabatically to $^2D(P)+^2S$(Li or Na) atomic states, and not to $^4S(P)+^2P$(Li or Na, $M_L=0$) states as we might have expected; the reason again is the intervening $^2D(P)$ state (Table 1). The equilibrium populations as obtained from the CAS wavefunction are

$$P-Li: 3s^{1.94}3p_{x,y}^{0.99}3p_z^{1.16}/2s^{0.48}2p_{x,y}^{0.00}2p_z^{0.38}$$

$$P-Na: 3s^{1.94}3p_{x,y}^{0.99}3p_z^{1.24}/3s^{0.43}3p_{x,y}^{0.00}3p_z^{0.31}$$

with ~0.1 and ~0.2 e^- transferred via the σ-frame to the P-atom of P-Li and P-Na respectively. The two π electrons are entirely localized on the P-atom, no delocalization to the p_x, p_y orbitals of the alkali atoms is observed. In addition, a significant sp_z hybridization on the Li and Na centers occurs, engendering a rather weak σ-bond, marked as σ^* in Table 2 and Table 3.

Admittedly, it is difficult to represent the bond formation of this state by a simple valence bond-Lewis diagram. A $^3\Sigma^-$ state tracing its ancestry to $^2D(P)+^2S(M)$ states can only be formed from the $M_s=0$ component of the $^2D(P)$ state,

$$|^2D, M_s=0\rangle = \{2|xy\bar{z}| - |\bar{x}yz| - |x\bar{y}z|\}$$
$$= \mathcal{A}(p_x p_y p_z)(2\alpha\alpha\beta - \beta\alpha\alpha - \alpha\beta\alpha).$$

Representing at equilibrium only the first part of the above wavefunction, the bond formation could be represented by the following picture similar of course to the $X^3\Sigma^-$ state.

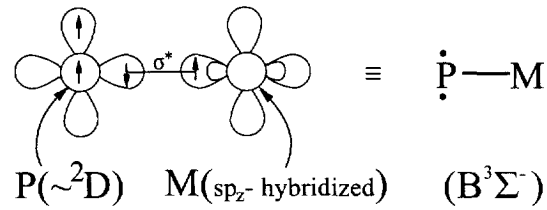

For both systems, the $B^3\Sigma^-$ state is the less ionic as compared with the rest of the states studied, and this is clearly reflected in the relatively small dipole moments, in Table 2 and Table 3, particularly for the P-Na molecule. In addition, and for both species, the dipole moment changes sign at the MRCI level, having its negative end toward the Li or Na atoms.

Finally, it is interesting to compare the $B^3\Sigma^-$ state of P-Li with the $B^3\Sigma^-$ of N-Li [5]. The morphologies of the two PECs are remarkably similar, but the N-Li correlates to $^4S(N)+^2P$(Li, $M_L=0$) atomic states as expected, due to the fact that the ^2P(Li) is *lower* in energy than the $^2D(N)$ state. In addition, although the calculated N-Li dipole moments for all states but the $B^3\Sigma^-$ are rather high (6–7 D), the latter is close to zero (0.02 D at the CISD level), in relative agreement with the $B^3\Sigma^-$ dipole moments of P-Li and P-Na systems.

4. Summary and conclusions

(1) Using CISD (+ corrections), CAS and CAS + 1 + 2 (+ corrections) methods, we have studied the electronic structure of P-Li and P-Na in their ground $^3\Sigma^-$ state and the low-lying excited $A^3\Pi$, $a^1\Delta$, $b^1\Sigma^+$ and $B^3\Sigma^-$ states. For all states full PECs are presented.

(2) With the exception of the $B^3\Sigma^-$ state, the states for both molecules show significant ionic character with approximately 0.4 e^- transferred from the Li or Na to the P atom and quite large dipole moments, 7.0–9.0 D.

(3) The energy seperations (T_e) of the two systems, with the exception of the $B^3\Sigma^-$ states, show a remarkable similarity; at the MRCI (MRCI + Q) level the two

T_e sets are as follows (kcal mol^{-1})

P–Li : 13.7(14.4), 20.0(20.7), 31.7(29.5), 52.3(52.1)

P–Na : 13.2(13.8), 21.1(22.0), 32.6(30.7), 44.2(42.7)

(4) In all absolute energies, E, there is an interesting agreement between the CISD + Q and MRCI + Q levels of theory, the largest difference being 6 mh for the $b^1\Sigma^+$ state of the P-Na system.

(5) For both molecules and for all states studied, the lone pair of the P atom (~3s) plays no role in the bonding mechanism, retaining a constant electron count of ~1.9 e^- at the CAS level.

References

[1] A. Mavridis, J.F. Harrison, J. Am. Chem. Soc. 102 (1980) 7651.
[2] K.F. Zmbov, C.H. Wu, Abstract of Proceedings of Symposium for the Year 1992 on Special Basic Research, 6 March 1993. Reported in Ref. [4].
[3] A.I. Boldyrev, J. Simons, J. Phys. Chem. 97 (1993) 6149.
[4] A.I. Boldyrev, J. Simons, R. von Schleyer, J. Chem. Phys. 99 (1993) 8793.
[5] S. Matsika, A. Papakondylis, A. Mavridis, Chem. Phys. Lett. 250 (1996) 409.
[6] T.H. Dunning Jr., J. Chem. Phys. 90 (1989) 1007.
[7] D.E. Woon, T.H. Dunning Jr., J. Chem. Phys. 98 (1993) 1358.
[8] P.-O. Widmark, B.J. Persson, B.O. Roos, Theor. Chim. Acta 79 (1991) 419.
[9] R. Shepard, I. Shavitt, R.M. Pitzer, D.C. Comeau, M. Pepper, H. Lischka, P.G. Szalay, R. Ahlrichs, F.B. Brown, J.-G. Zhao, Int. J. Quantum Chem. S22 (1988) 149.
[10] E.R. Davidson, MELD, Department of Chemistry, Indiana University, Bloomington, IN, 1991.
[11] C.E. Moore, Atomic energy levels, in: Natl. Stand. Ref. Data Ser., U.S. Natl. Bur. Stand., Cir. 35, 1973.
[12] E.R. Davidson, in: R. Daudel, B. Pullman (Eds.), The World of Quantum Chemistry, Reidel, Dordrecht, 1974.
[13] M.R.A. Blomberg, P.E.M. Siegbahn, J. Chem. Phys. 78 (1983) 5682.